Regulation of Nicotine Biosynthesis by an Endogenous Target Mimicry of MicroRNA in Tobacco[1][OPEN]

Fangfang Li[2], Weidi Wang[2], Nan Zhao, Bingguang Xiao, Peijian Cao, Xingfu Wu, Chuyu Ye, Enhui Shen, Jie Qiu, Qian-Hao Zhu, Jiahua Xie, Xueping Zhou*, and Longjiang Fan*

Institute of Crop Science and Research Center for Air Pollution and Health (F.L., W.W., N.Z., C.Y., E.S., J.Q., L.F.) and Institute of Biotechnology (F.L., N.Z., X.Z.), Zhejiang University, Hangzhou 310058, China; Yunnan Academy of Tobacco Agricultural Sciences and China Tobacco Breeding Research Center at Yunnan, Yuxi 653100, China (B.X., X.W.); National Center of Tobacco Genes, Zhengzhou 450001, China (P.C.); Commonwealth Scientific and Industrial Research Organization Agriculture Flagship, Canberra, Australian Capital Territory 2601, Australia (Q.-H.Z.); and Department of Pharmaceutical Sciences, North Carolina Central University, Durham, North Carolina 27707 (J.X.)

ORCID IDs: 0000-0002-1791-4461 (B.X.); 0000-0001-9991-423X (P.C.); 0000-0003-0903-0356 (C.Y.); 0000-0002-6505-7417 (Q.-H.Z.); 0000-0001-7695-7958 (L.F.).

The interaction between noncoding endogenous target mimicry (eTM) and its corresponding microRNA (miRNA) is a newly discovered regulatory mechanism and plays pivotal roles in various biological processes in plants. Tobacco (*Nicotiana tabacum*) is a model plant for studying secondary metabolite alkaloids, of which nicotine accounts for approximately 90%. In this work, we identified four unique tobacco-specific miRNAs that were predicted to target key genes of the nicotine biosynthesis and catabolism pathways and an eTM, novel tobacco miRNA (nta)-eTMX27, for nta-miRX27 that targets *QUINOLINATE PHOSPHORIBOSYLTRANSFERASE2* (*QPT2*) encoding a quinolinate phosphoribosyltransferase. The expression level of nta-miRX27 was significantly down-regulated, while that of *QPT2* and nta-eTMX27 was significantly up-regulated after topping, and consequently, nicotine content increased in the topping-treated plants. The topping-induced down-regulation of nta-miRX27 and up-regulation of *QPT2* were only observed in plants with a functional nta-eTMX27 but not in transgenic plants containing an RNA interference construct targeting nta-eTMX27. Our results demonstrated that enhanced nicotine biosynthesis in the topping-treated tobacco plants is achieved by nta-eTMX27-mediated inhibition of the expression and functions of nta-miRX27. To our knowledge, this is the first report about regulation of secondary metabolite biosynthesis by an miRNA-eTM regulatory module in plants.

MicroRNAs (miRNAs) are a class of small noncoding RNAs with a typical length of 20 to 22 nucleotides and have been shown to play important roles in development, signal transduction, and responses to biotic and abiotic stresses in plants (Phillips et al., 2007; Khraiwesh et al., 2012). MiRNAs are generated from single-strand RNA precursors (pre-miRNAs) with a stem-loop structure (Bartel, 2004). The pre-miRNA stem-loop structures are processed into miRNA/miRNA* duplexes by a protein complex including Dicer-like1 (a ribonuclease [RNase] III-like endoribonuclease). The mature miRNA is then loaded onto the Argonaute-containing RNA-induced silencing complex to cause target mRNA degradation or translational repression through complementary sequence binding (Naqvi et al., 2012). Most plant miRNAs have perfect or near-perfect complementarity with their targets (Axtell and Bowman, 2008; Mallory and Bouché, 2008); therefore, plant miRNA targets can usually be successfully predicted based on sequence complementarity between miRNAs and their targets (Rhoades et al., 2002; Sunkar and Zhu, 2004). A perfect base pairing between miRNAs and their targets at the ninth to 11th positions from the 5′ end of miRNAs is important for effective miRNA-mediated cleavage of targets (Jones-Rhoades et al., 2006; Pasquinelli, 2012).

In Arabidopsis (*Arabidopsis thaliana*), a long nonprotein-coding mRNA gene, *INDUCED BY PHOSPHATE STARVTION1* (*IPS1*), was found to be bound by miR399 with a three-nucleotide bulge in the middle of the miR399 binding site. This central mismatch disrupts crucial

[1] This work was supported by Yunnan Provincial Tobacco Company (grant no. 2011YN04 to L.F.), the National Natural Science Foundation of China (grant no. 31060046 to B.X.), and the Post-Doctoral Science Foundation of China (grant no. 2015M570514 to F.L.).

[2] These authors contributed equally to the article.

* Address correspondence to fanlj@zju.edu.cn and zzhou@zju.edu.cn.

The author responsible for distribution of materials integral to the findings presented in this article in accordance with the policy described in the Instructions for Authors (www.plantphysiol.org) is: Longjiang Fan (fanlj@zju.edu.cn).

F.L. performed all of the molecular biology experiments, analyzed the data, and wrote the article; N.Z., X.W., and B.X. performed the transgenic plants and nicotine measurements; W.W., P.C., C.Y., E.S., and J.Q. contributed to the sequence analysis; Q.-H.Z. analyzed the data and revised the article; J.X. discussed the data; L.F. and X.Z. conceived the project and revised the article.

[OPEN] Articles can be viewed without a subscription.

www.plantphysiol.org/cgi/doi/10.1104/pp.15.00649

base pairing between miR399 and *IPS1* and hence inhibits miR399-mediated cleavage of *IPS1*. This observation leads to the hypothesis that *IPS1* functions as a noncleavable endogenous target mimicry (eTM) of miR399, which blocks the interaction between miR399 and its authentic targets by sequestering miR399 and arresting its cleavage activity (Franco-Zorrilla et al., 2007). Later, noncoding eTMs for diverse miRNAs have been identified in Arabidopsis, rice (*Oryza sativa*), and soybean (*Glycine max*), and some of them have been shown to regulate plant development by repressing miRNA function (Todesco et al., 2010; Ivashuta et al., 2011; Wu et al., 2013). These studies also suggested that eTMs are widespread in plant species. Recent studies based on transcriptome sequencing have demonstrated the widespread existence of long noncoding RNAs in plants (Li et al., 2014b; Zhang et al., 2014); however, functions of the majority of those long noncoding RNAs are largely unknown. It would not be surprising to find a portion of these long noncoding RNAs acting as eTMs. Additionally, short tandem target mimic (STTM) technology has been developed with an aim to investigate functions of small RNAs by blocking small RNA functions in plants and animals (Tang et al., 2012a; Yan et al., 2012). STTM is a powerful technology complementing the target mimic in plants and the miRNA sponge in animals.

Alkaloids are a major type of secondary metabolites. Nicotine accounts for approximately 90% of the total alkaloid content and serves as defensive compounds against herbivores in tobacco (*Nicotiana tabacum*; Saitoh et al., 1985; Baldwin et al., 2001). Meanwhile, nicotine is also the most important component in tobacco products due to its stimulatory and addictive effects. Nicotine is exclusively synthesized in tobacco roots and then transported to leaves through the xylem (Dewey and Xie, 2013). Nicotine alkaloids are accumulated in most *Nicotiana* species (Baldwin, 1999). The nicotine biosynthesis and catabolism pathways have been extensively studied (for review, see Dewey and Xie, 2013). Several key genes encoding enzymes of the nicotine biosynthesis pathway, such as quinolinate phosphoribosyltransferase (QPT), putrescine methyltransferase (PMT), *N*-methylputrescine oxidase, and nicotine *N*-demethylase (a cytochrome P450 monooxygenase [CYP82E4]), have been cloned and characterized (Conkling et al., 1990; Hibi et al., 1992; Siminszky et al., 2005; Katoh et al., 2006; Heim et al., 2007). QPT converts quinolinic acid to nicotinic acid mononucleotide and serves as the entry point into the pyridine nucleotide cycle that leads to the production of nicotinic acid and consequently nicotine (Dewey and Xie, 2013). QPT was first isolated from tobacco roots by Conkling et al. (1990) and later characterized by Song (1997) and Sinclair et al. (2000). *QPT2* is strongly and exclusively expressed in root tissue and involved in nicotine biosynthesis, while its homolog *QPT1* is nonresponsive to biotic and abiotic stresses and retains its original function in NAD production (Dewey and Xie, 2013). Transgenic tobacco lines with a low level of nicotine content have been developed by suppression of *QPT2* using the antisense-mediated gene-silencing approach (Xie et al., 2004).

Recent reports have shown that miRNAs are involved in regulation of secondary-metabolite synthesis in plants. For example, miR163 can change the production profiles of secondary metabolite in Arabidopsis (Ng et al., 2011); miR393 redirects the secondary-metabolite productions via perturbing auxin signaling (Robert-Seilaniantz et al., 2011); and some miRNAs might be involved in biosynthesis of benzylisoquinoline alkaloids in opium poppy (*Papaver somniferum*; Boke et al., 2015). In tobacco, it has been shown that miR164 and its target *NtNAC-R1*, a unique NAC (for NAM, no apical meristem) transcription factor identified in tobacco, was down- and up-regulated in response to topping, respectively, and resulted in increase of lateral roots and nicotine contents (Fu et al., 2013). However, it is still unclear whether miRNAs are directly involved in regulation of the nicotine biosynthesis pathway in tobacco.

To determine the roles of miRNAs in nicotine biosynthesis, in this study, we first identified nicotine biosynthesis-related miRNAs in two small RNA populations generated from topping-treated tobacco roots using the newly available tobacco genome sequence as a reference (Sierro et al., 2014). We found four unique miRNAs that target several key genes of the nicotine biosynthesis and catabolism pathways. Further investigation on novel tobacco miRNA (nta)-miRX27, which targets *QPT2*, by overexpression and inhibition of the miRNA function confirmed that nta-miRX27 played an important role in regulation of tobacco plants in response to topping and nicotine accumulations. More interestingly, we identified an eTM (nta-eTMX27) for nta-miRX27 and proved that it can effectively inhibit the functions of nta-miRX27 and regulate nicotine biosynthesis in the topping-treated tobacco plants.

RESULTS

Identification of Nicotine Biosynthesis-Related miRNAs in Tobacco

The recently available genome sequences of tobacco and its two progenitors provided an opportunity to identify miRNAs related to nicotine biosynthesis in tobacco. Based on the small-RNA data generated from roots of control and topping-treated tobacco plants by deep sequencing in our previous study (Tang et al., 2012b), we identified a number of unique miRNAs that have not been reported previously, including four that were predicted to target genes (*QPT1*, *QPT2*, *PMT2*, and *CYP82E4*) involved in nicotine biosynthesis (Fig. 1A; Supplemental Table S1). These four miRNAs seemed to be tobacco specific, as no homologous sequence was found in the miRBase database.

Previous studies demonstrated that there was a significant increase in the activity of several nicotine biosynthetic enzymes in the tobacco roots at 24 to 48 h after topping (Dewey and Xie, 2013). To test the effects of

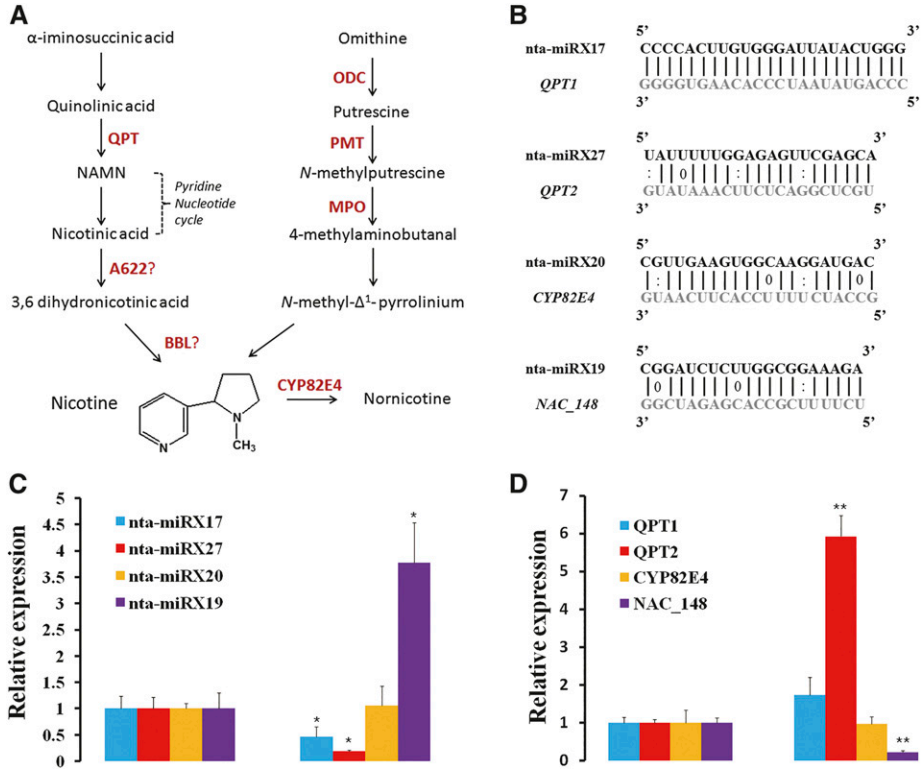

Figure 1. Genes involved in nicotine biosynthesis in tobacco and expression changes of miRNAs and their nicotine-related targets at 48 h after topping. A, A schematic diagram of the nicotine biosynthesis pathway in tobacco (adapted from Dewey and Xie, 2013). A622, Isoflavone reductase-like protein; BBL, berberine bridge enzyme-like; MPO, *N*-methylputrescine oxidase; CYP82E4, nicotine *N*-demethylase; ODC, Orn decarboxylase. B, Alignment of nta-miRNAs and their targets. Base pairing between miRNA and its target are shown, in which a vertical line means a Watson-Crick pair, two dots represent a G-U pair, and 0 means a mismatch. C, RT-qPCR analyses of nta-miRX17, nta-miRX27, nta-miRX20, and nta-miRX19 at 48 h after topping. Mitochondrial 5S RNA served as an internal standard for expression normalization. D, RT-qPCR analyses of miRNA target genes (*QPT1*, *QPT2*, *CYP83E4*, and *NAC_148*) at 48 h after topping. *Glyceraldehyde 3-phosphate dehydrogenase* mRNA served as an internal standard for expression normalization. Three independent experiments, each consisting of three control and topping-treated plants, were carried out for quantification analyses, and representative results in one time are presented. The expression levels of miRNAs and their targets in plants without topping treatment (control) are arbitrarily set as 1. Error bars indicate SD. Student's *t* tests were performed to compare differences of miRNAs and their targets between the control and the topping treatment. A single asterisk indicates a significant difference ($P < 0.05$), and double asterisks indicate a highly significant difference ($P < 0.01$) between the two paired samples.

topping on nicotine biosynthesis-related miRNAs and their target genes, we measured their expression changes, as well as *NtNAC_148* (targeted by nta-miRX19), which has been shown to be down-regulated upon topping treatment (W. Wang and L. Fan, unpublished data), using samples collected at 48 h after topping. As expected, *NAC_148* was down-regulated significantly after topping, which is most likely caused by up-regulation of nta-miRX19 (Fig. 1, B and C). The expression levels of nta-miRX17 and nta-miRX27 were down-regulated upon topping, and consequently, their targets *QPT1* and *QPT2* were up-regulated (Fig. 1, C and D). The negatively correlated relationship was striking for nta-miRX27 and *QPT2* (Fig. 1, C and D). By contrast, topping seemed to have no effect on the expression of nta-miRX20, nta-miRX13, and their targets, *CYP82E4* and *PMT2*, respectively. *CYP82E4*, which is responsible for nicotine to nornicotine demethylation (Dewey and Xie, 2013), has been shown to not be topping responsive. These results suggested that the nta-miRX27-*QPT2* interaction may be important for regulation of nicotine biosynthesis in tobacco.

The reversely correlated expression relationship between nta-miRX27 and its target *QPT2* suggests nta-miRX27-mediated cleavage of *QPT2*. Two binding sites of nta-miRX27 could be predicted on the *QPT2* gene. The first one is located at exon number 2, and the second one is located at the intron between exon numbers 8 and 9 (based on AJ748263 deposited in the National Center for Biotechnology Information) or at exon number 8 (based on Fgenesh prediction; http://www.softberry.com). We used RNA ligase-mediated (RLM)-5′ RACE to confirm nta-miRX27-mediated cleavage of *QPT2* but failed for both sites (Supplemental Fig. S1), although the first one was confirmed to be cleaved based on our previous degradome data (Supplemental Fig. S2)

Regulation of nta-miRX27 on Endogenous *QPT2* Expression and Nicotine Accumulation

To investigate whether nta-miRX27 functions to repress expression of its target *QPT2* and plays any role in nicotine production, we generated transgenic tobacco plants overexpressing or silencing nta-miRX27. The silencing transgenic plants (nta-STTMX27) were generated using the STTM strategy (Fig. 2A). The expression levels of nta-miRX27 in the overexpressing and silencing transgenic plants were confirmed to be significantly up- and down-regulated, respectively (Fig. 2C). The expression changes of nta-miRX27 in all transgenic plants did not cause observable phenotypic changes (Fig. 2B), consistent with the expected effects of nta-miRX27. The expression level of *QPT2* was decreased by approximately 50% in the nta-miRX27 transgenic plants compared with the control plants, but a significantly increased level of *QPT2* was observed in the nta-STTMX27 transgenic plants (Fig. 2C). Consistent with these expression changes of *QPT2*, decreased and increased nicotine contents were observed in the nta-miRX27 and nta-STTMX27 transgenic plants, respectively. The nicotine content in the leaves of the nta-STTMX27 and nta-miRX27 transgenic plants was 9.17 ± 1.29 mg g^{-1} and 2.17 ± 1.15 mg g^{-1}, respectively (Fig. 2D). These results strongly suggested that nta-miRX27-mediated regulation of its target *QPT2* plays an important role in nicotine biosynthesis in tobacco.

Identification and Expression Analysis of eTMs for nta-miRX27

To determine potentially additional regulators related to the nat-miRX27-*QPT2* module involved in regulation of nicotine biosynthesis, we performed eTM identification using various available transcripts, including those in-house assembled using available tobacco RNA sequencing data, and identified an eTM for nta-miRX27, which was named nta-eTMX27. The putative transcript of nta-eTMX27 was 1,213 bp long, with the largest predicted open reading frame being 144 bp in length. It was covered by several ESTs (FS399281, FS416548, and FG201217), and at least one EST (FG201217) covered the target mimic site of nta-eTMX27, although a few single-nucleotide polymorphisms were found between

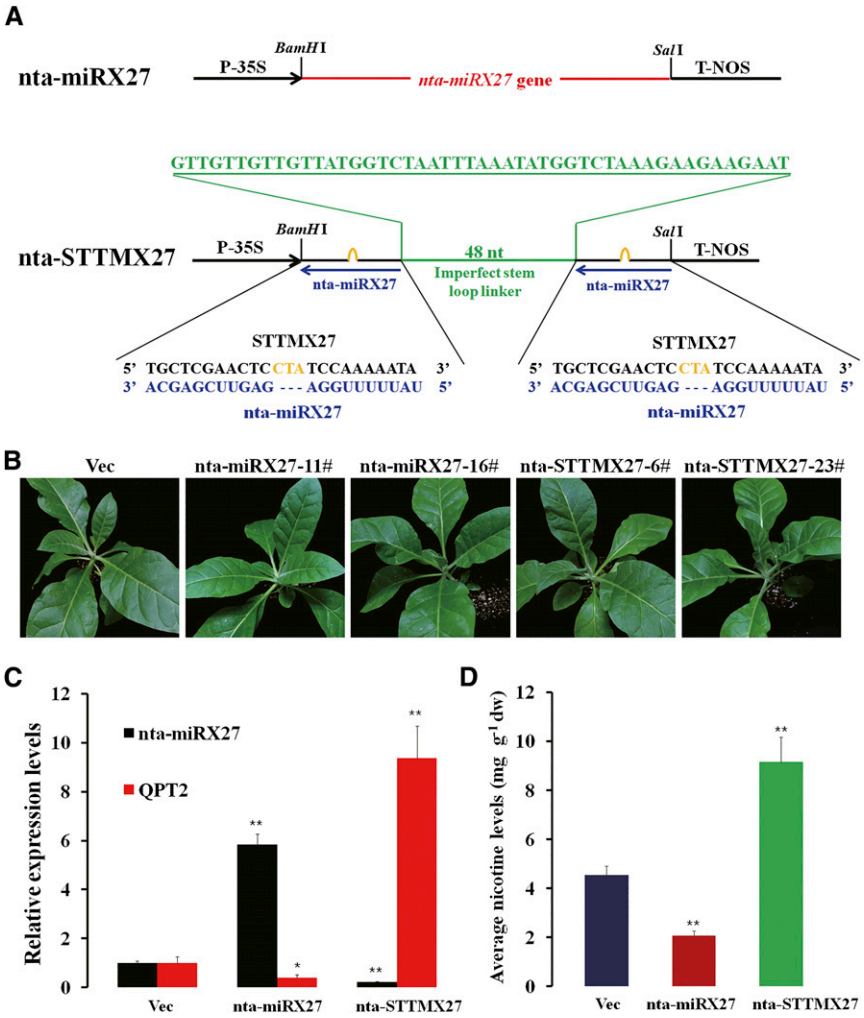

Figure 2. nta-miRX27 repressed *QPT2* expressions and reduced nicotine contents. A, Diagram of nta-miRX27 and nta-STTMX27 structures showing the design strategy. nta-miRX27 gene and two tandem target mimics (STTMX27) spaced by a 48-nucleotide (nt) imperfect stem-loop linker were cloned between a *Cauliflower mosaic virus* 35S promoter (P-35S) and nopaline synthase (NOS) terminator (T-NOS) to produce nta-miRX27 and nta-STTMX27 constructs, respectively. Red indicates the nta-miRX27 gene, green indicates the spacer region and the spacer sequence, blue indicates the mature nta-miRX27 sequences, and orange indicates the bulge sequences in the miRNA binding sites. B, Phenotypes of 30-d-old transgenic plants containing nta-miRX27 or nta-STTMX27 compared with that of plants transformed with a Vec. Two independent and representative transgenic lines overexpressing nta-miRX27 (nta-miRX27-11# and nta-miRX27-16#) and silencing nta-miRX27 (nta-STTMX27-6# and nta-STTMX27-23#) are shown. C, Relative expression levels of nta-miRX27 and its target gene *QPT2* in nta-miRX27 and nta-STTMX27 transgenic plants compared with that of the Vec plants. Three individual plants per genotype were used in RT-qPCR, and bars represent SD of three replicates. D, Average nicotine contents in leaves sampled from the Vec, nta-miRX27, and nta-STTMX27 plants. Each mean value was derived from three independent experiments ($n = 9$). Error bars indicate the SD of three replicates. Significance tests were performed by the Student's *t* test. A single asterisk indicates a significant difference ($P < 0.05$), and double asterisks indicate a highly significant difference ($P < 0.01$) between the two paired samples. dw, Dry weight.

nta-eTMX27 and FG201217. The binding site of nta-miRX27 in nta-eTMX27 contains a three-nucleotide bulge between the ninth and 10th positions of nta-miRX27 (Fig. 3A). Moreover, according to the degradome data generated previously (Tang et al., 2012b), no degradomic read was mapped to the target mimic site of nta-eTMX27, supporting the notion that nta-eTMX27 may act as a decoy for nta-miRX27. Nta-eTMX27 was found to be expressed in root, stem, and leaf tissues but not in flowers (Fig. 3B).

To determine whether the predicted nta-eTMX27 plays a role in repressing miRNA function, its expression changes together with that of nta-miRX27 and its target *QPT2* were analyzed in roots of the tobacco plants sampled at 3 to 48 h after the topping treatment (Fig. 3C). Apparently, the expression level of nta-eTMX27 increased steadily after the topping treatment and was approximately 9-fold higher than that of the control (0 h after topping) at 48 h after the topping treatment (Fig. 3C, first column). Similarly, the expression level of *QPT2* was also up-regulated after topping (Fig. 3C, second column), while the expression level of nta-miRX27 was down-regulated during the same time period after the topping treatment (Fig. 3C, third column). These results indicate that topping treatment induces nta-eTMX27 expression, which leads to down-regulation of nta-miRX27 and an increase of *QPT2* expression.

nta-eTMX27 Induced miRNA Degradation and Repressed miRNA Function

To confirm the function of nta-eTMX27, i.e. sequestration of nta-miRX27 away from its target *QPT2*, we generated transgenic tobacco plants overexpressing nta-eTMX27 or harboring a RNA interference (RNAi) construct (double-stranded [ds]-nta-eTMX27) targeting nta-eTMX27. Under the greenhouse conditions, all transgenic plants grew normally and did not show obvious altered phenotypes compared with the plants transformed with the empty vector (Vec; Fig. 4A). Real-time (RT) quantitative PCR (qPCR) assay showed that the expression level of nta-eTMX27 was approximately 3-fold higher in the nta-eTMX27 overexpressing lines than in the Vec lines, while the expression levels of nta-miRX27 and *QPT2* were reduced by approximately 50% and increased by more than 2-fold, respectively (Fig. 4B). In the nta-eTMX27 RNAi transgenic plants (ds-nta-eTMX27), the expression level of nta-eTMX27 was reduced to approximately 23% of the level in the Vec plants. As a result, the expression levels of nta-miRX27 and *QPT2* were increased and decreased, respectively (Fig. 4B). In addition, the nicotine contents in the nta-eTMX27 and ds-nta-eTMX27 transgenic lines were significantly increased and decreased, respectively (Fig. 4C). These results not only confirmed the regulatory module involving nta-miRX27, *QPT2*, and nta-eTMX27, but also indicate that the nicotine contents in tobacco plants can be manipulated by overexpression or silencing of nta-eTMX27.

The opposite functions of nta-miRX27 and nta-eTMX27 in regulating *QPT2* transcript levels and nicotine biosynthesis led us to postulate that nta-eTMX27 may induce nta-miRX27 degradation and repress miRNA function in response to external stimuli, such as topping, during plant growth and development. To test this possibility, we compared the expression changes of nta-miRX27 and *QPT2* in the transgenic plants containing the Vec or ds-nta-eTMX27 construct after the topping treatment. As expected, expression of nta-miRX27 was down-regulated, while expression of *QPT2* and nta-eTMX27 was up-regulated in the Vec plants (Fig. 4, D–F); however, these changes were not observed in the ds-nta-eTMX27

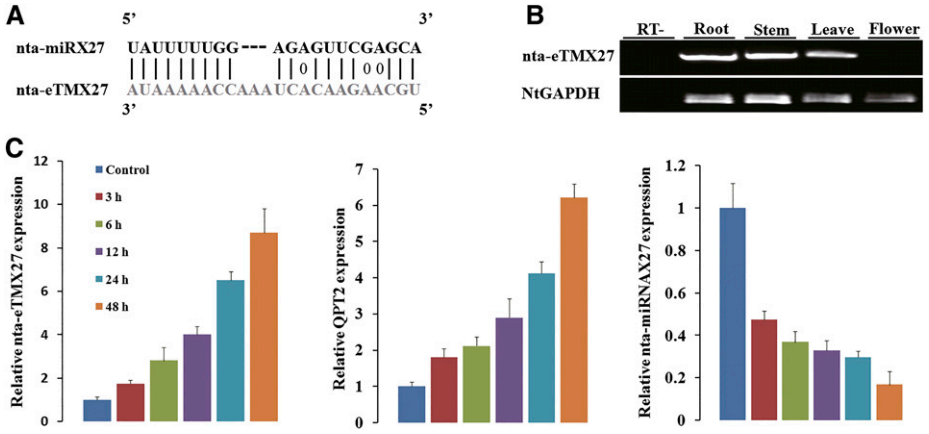

Figure 3. Topping-induced expression of endogenous nta-eTMX27 in tobacco root. A, The predicted base-pairing pattern between nta-miRX27 and its eTM nta-eTMX27. B. Semiquantitative RT-PCR analysis of expressions of nta-eTMX27 in four tissues. *Tobacco glyceraldehyde 3-phosphate dehydrogenase* gene (*NtGAPDH*) was used as control. RT– represents RT negative control, i.e. RT without reverse transcriptase. C, The relative transcription levels of nta-eTMX27, *QPT2*, and nta-miRX27 in tobacco root tissues measured at 3, 6, 12, 24, and 48 h after topping. Three independent experiments, each consisting of three control and topping-treated plants, were carried out for quantification analyses, and representative results in one time are presented. The expression level at the 0-h time point (control) was arbitrarily set as 1. Error bars indicate the SD.

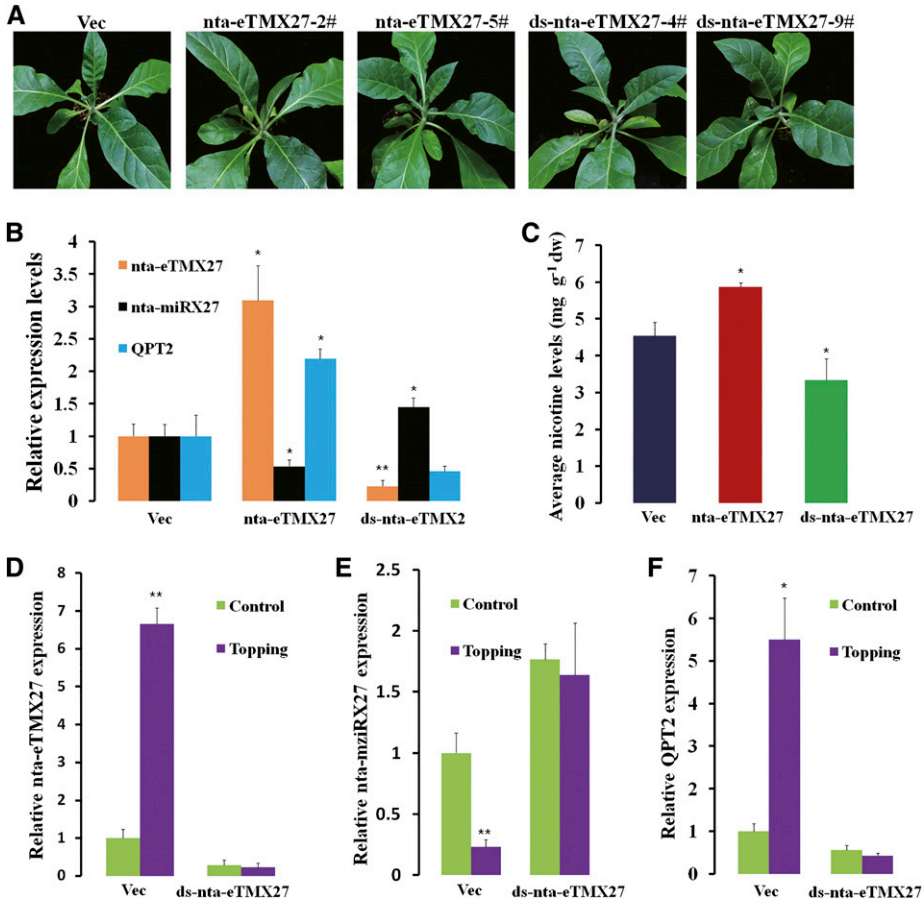

Figure 4. Functional analyses of nta-eTMX27. A, Phenotypes of nta-eTMX27 overexpression and silencing plants. Two independent and representative transgenic lines overexpressing nta-eTMX27 (nta-eTMX27-2# and nta-eTMX27-5#) and silencing nta-eTMX27 (ds-nta-eTMX27-4# and ds-nta-eTMX27-9#) are shown. B, Relative expression levels of nta-eTMX27, nta-miRX27, and *QPT2* in nta-eTMX27-overexpressing and -silencing transgenic plants compared with that of the Vec plants. Three individual plants per genotype were used in RT-qPCR. Bars show SD. C. Average leaf nicotine contents of the Vec, nta-miRX27, and nta-STTMX27 lines. A single asterisk indicates a significant difference ($P < 0.05$) between the nta-miRX27 or nta-STTMX27 line and the Vec control. Error bars indicate the SD. dw, Dry weight. D, Expression levels of nta-eTMX27 in roots of transgenic plants transformed with the Vec or ds-nta-eTMX27 construct in response to topping. Samples were collected at 48 h after topping treatment (without topping as control). The expression level in the Vec plants without topping treatment was arbitrarily set as 1. Error bars indicate SD. Double asterisks indicate a significant difference (Student's *t* test, $P < 0.01$) between the two samples. E, Relative expression levels of nta-eTMX27 in roots of transgenic plants transformed with the Vec or ds-nta-eTMX27 after topping treatment at 48 h. The expression level of the Vec plants with control treatment was arbitrarily set as 1. Error bars indicate the SD. F, Relative expression levels of *QPT2* in the Vec and ds-nta-eTMX27 transgenic plants after topping treatment at 48 h. Error bars indicate SD. The expression level of the Vec plants with control treatment was arbitrarily set as 1. A single asterisk indicates a significant difference (Student's *t* test, $P < 0.05$), and double asterisks indicate a highly significant difference (Student's *t* test, $P < 0.01$) between the two paired samples.

transgenic plants (Fig. 4, D–F). These results indicate that nta-eTMX27 seems to be essential for topping-induced down-regulation of nta-miRX27 and that nta-eTMX27 may play a role in repressing the function of nta-miRX27 by degradation under stress conditions.

Evolution of nta-miRX27 and nta-eTMX27

No ortholog of the primary transcript of nta-miRX27 or the nta-miRX27 mature sequence could be found in the current tomato genome (http://www.solgenomics.net/) and miRBase, suggesting that nta-miRX27 may be *Nicotiana* spp. specific. A near-identical sequence of nta-miRX27 was found in *Nicotiana sylvestris* but not in *Nicotiana tomentosiformis* (Fig. 5A), suggesting that nta-miRX27 was most likely derived from the progenitor *N. sylvestris*. Meanwhile, *QPT2* of common tobacco also showed more sequence similarity, including the presence of the nta-miRX27 binding site, with its ortholog in *N. sylvestris*. By contrast, no miRNA and miRNA target site could be predicted in the ortholog of *QPT2* and its surrounding region in *N. tomentosiformis* because of nucleotide mutations, implying that the nta-miRX27-*QPT2*

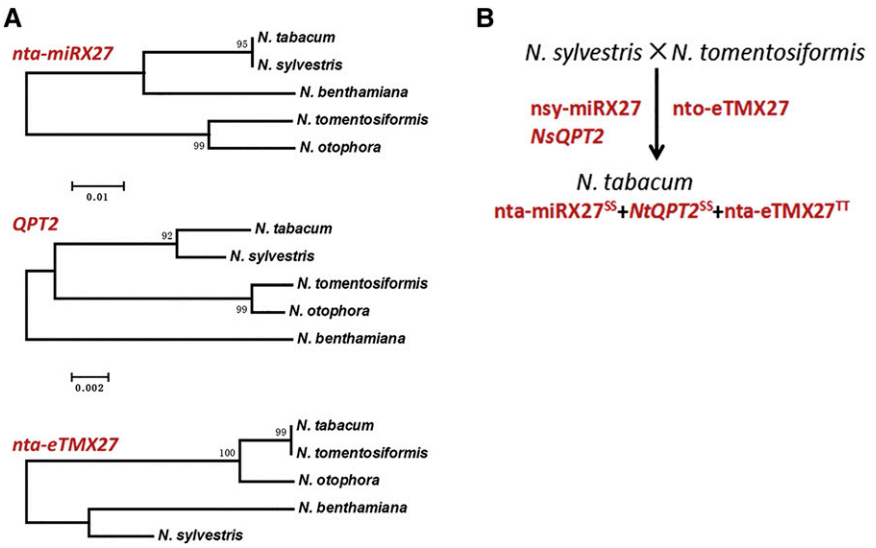

Figure 5. Phylogenetic tree (A) and evolution model (B) of nta-miRX27, its target *QPT2*, and target mimic nta-eTMX27 in the *Nicotiana* genus. The nucleotide sequences of nta-miRX27, *QPT2*, and nta-eTMX27 from tobacco, *N. sylvestris* (nsy), *N. benthamiana*, *N. otophora*, and *N. tomentosiformis* (nto) were aligned using the neighbor-joining method with 1,000 replications.

regulatory module might have been only evolved in the progenitor *N. sylvestris* but not in *N. tomentosiformis*. Interestingly, an almost identical sequence of nta-eTMX27 was found in *N. tomentosiformis* but not in *N. sylvestris* (Fig. 5A). Compared with common tobacco and *N. tomentosiformis*, *N. sylvestris* had one nucleotide substitution and an insertion/deletion in the target mimic site of the sequence corresponding to nta-eTMX27 (data not shown). Consequently, the nta-miRX27-nta-eTMX27 interaction could not be predicted in the *N. sylvestris* genome based on our current bioinformatic pipeline.

DISCUSSION

The role of miRNAs in secondary metabolite biosynthesis has been demonstrated in plants (Ng et al., 2011; Robert-Seilaniantz et al., 2011), and potential regulation of alkaloid biosynthesis by miRNA in opium poppy has also been suggested (Boke et al., 2015). Target mimicry has emerged as a new mechanism regulating function of miRNAs, and a number of long noncoding RNAs acting as eTMs to block the biological function of miRNAs have been identified in plants (Franco-Zorrilla et al., 2007; Todesco et al., 2010; Ivashuta et al., 2011; Meng et al., 2012; Wu et al., 2013; Ye et al., 2014). In Arabidopsis, in addition to *IPS1*, the first validated functional eTM in plants, eTMs for miR160 and miR166 have also been shown to play an important role in regulation of plant development, which was possibly achieved by eTM-induced miRNA degradation (Wu et al., 2013). In this study, we showed evidence that topping could induce the expression changes of nicotine-related miRNAs and their targets. For example, the expression levels of nta-miRX27 and its target *QPT2*, one of the key genes of the nicotine biosynthesis pathway, were down- and up-regulated in the topping-treated tobacco plants, respectively. Using transgenic plants overexpressing or silencing nta-miRX27, we demonstrated that nta-miRX27 directly regulates expression of *QPT2* and, consequently, the accumulation of nicotine. Furthermore, we identified a long noncoding RNA, i.e. nta-eTMX27, which contains a noncleavable nta-miRX27 binding site. Similar to *QPT2*, the expression of nta-eTMX27 was induced in response to topping. As reported previously in other plant species (Wu et al., 2013), topping-induced down-regulation of nta-miRX27 and up-regulation of *QPT2* in tobacco observed in this study (Fig. 3C) might be a result of nta-miRX27 degradation caused by up-regulated nta-eTMX27. This notion was confirmed using transgenic plants containing a hairpin construct targeting nta-eTMX27, in which no topping-induced down-regulation of nta-miRX27 and up-regulation of *QPT2* were observed. Our results demonstrated a crucial role of nta-eTMX27 in regulation of nicotine biosynthesis by acting as a decoy of nta-miRX27 to sequester and degrade nta-miRX27. To our knowledge, this is the first report showing that eTM played a role in biosynthesis of secondary metabolites in plants.

Two binding or cleavage sites of nta-miRX27 were predicted on the *QPT2* gene with a predicted targeting score of 4.5 and 2.5, respectively. The first predicted binding site at exon number 2 was confirmed by degradome data (Supplemental Figs. S1 and S2); however, our further RLM-RACE experiments failed to confirm nta-miRX27-mediated cleavage at both sites. We repeated the RLM-RACE experiment a couple of times with different primers. For the second binding site, we used primers based on both the complementary DNA (cDNA) and the intron sequence downstream of the predicted binding site, which is located at an intron based on the *QPT2* gene (AJ748263) deposited in the National Center for Biotechnology Information. For both sites, the RLM-RACE products were mapped to the flanking regions of the predicted cleavage sites of nta-miRX27 but not at the predicted cleavage sites (Supplemental Fig. S1). The distribution pattern of the 5′ ends of the RACE products suggests that the clones we sequenced are randomly degraded products, although similar distribution pattern of 5′ RACE products

has been observed for some conserved but lowly expressed miRNAs (Shen et al., 2014; Chen et al., 2015). We cannot rule out the possibility that we failed to amplify and clone the right cleavage products due to technical issue, but it is most likely that the fragmented *QPT2* resulting from nta-miRX27-mediated cleavage is very susceptible to degradation induced by RNA decay proteins such as nuclear exoribonucleases (5′-3′) and the exosome complex (3′-5′). In addition, we cannot exclude the possibility that nta-miRX27 targets unprocessed *QPT2* in the nucleus, because the second predicted nta-miRX27 binding site is located at the intron of alternatively spliced *QPT2*. If that is the case, nta-miRX27 could be involved in regulation of *QPT2* by interfering its splicing and/or mRNA maturation. Whatever the possible reason for the negative RACE result, the results observed in transgenic plants clearly suggest that the transcript level of *QPT2* is regulated by nta-miRX27. Nevertheless, it is in our interest to perform further experiments to find out the mechanism underlying nta-miRX27-mediated regulation of *QPT2*.

Among various approaches for functional characterization of miRNAs, STTM technology has received more attention due to its high efficiency in suppressing miRNA functions using the target mimicry mechanism (Yan et al., 2012). In our work, overexpression of nta-STTMX27 could reduce the nta-miRX27 levels to approximately 20% of the control levels and produced transgenic lines with the highest contents of nicotine in this study. This result confirmed the efficiency of the technology and also suggested that nta-miRX27 played an important role in nicotine biosynthesis. Transgenic plants overexpressing and silencing nta-eTMX27 showed increased and reduced accumulation of nicotine, respectively, which was consistent with its function in repressing nta-miRX27 and facilitating expression of *QPT2*.

Common tobacco is a model plant organism for studying diverse fundamental biological processes, such as disease susceptibility and secondary metabolites. Tobacco has rich secondary metabolites (>4,000 chemical components) and prompted numerous studies on biologically active metabolic substances (Sierro et al., 2014). For example, the alkaloid biosynthesis pathway received a large amount of attention from scientists and has been well studied over the past 30 years (Dewey and Xie, 2013). A gene network including more than 10 nodes or protein-coding genes has been characterized for the pathway. Recent studies indicated that some transcription factors, such as *NAC*, *ETS2 Repressor Factor*, and *MYC*, might also be indirectly involved in alkaloid biosynthesis via regulating plant hormones (Zhang et al., 2012; Fu et al., 2013). In this study, an additional regulator, i.e. a noncoding RNA acting as an miRNA or miRNA decoy, was demonstrated to be directly involved in regulation of the key genes of the alkaloid biosynthesis pathway. We believe that more such noncoding genes will be identified for the pathway in the future. In this sense, our study opened a new channel for investigation of the genetic network related to alkaloid biosynthesis in plants.

Modern tobacco is a natural amphidiploid whose genomes originated from the hybridization of two wild progenitors, *N. tomentosiformis* and *N. sylvestris* (Dewey and Xie, 2013). It is a relatively new species but experienced a dramatic domestication selection after the hybridization of two progenitors. For example, over time, loss-of-function mutations in the major nicotine demethylase genes have been selected that enabled modern tobacco to accumulate nicotine rather than nornicotine (Gavilano et al., 2007). By contrast, the normal demethylase genes in the two progenitors made them accumulate a higher level of nornicotine content but not nicotine. According to our phylogenetic analysis results, we believe that the regulatory module of nta-miRX27-*QPT2*-nta-eTMX27 was only evolved in tobacco after the hybridization of its two progenitors, *N. tomentosiformis* and *N. sylvestris*, but not in the progenitors themselves (Fig. 5B). *QPT2* plays a key role in biosynthesis of nicotine, one of the main agronomic traits in tobacco under artificial selection. Evolution of the nta-eTMX27-nta-miRX27-*QPT2* regulatory module in modern tobacco could be driven by domestication and, subsequently, intensive genetic improvement that aimed to increase the nicotine content.

MATERIALS AND METHODS

Plant Materials and Treatment

All root samples were collected from tobacco (*Nicotiana tabacum*) 'Hicks Broad.' Tobacco plants were grown at 25°C and 65% humidity in a growth chamber with 16 h of light and 8 h of dark. At least three 60-d-old (days after seeding) plants were used for topping treatment, and plants with a similar size without topping treatment were used as control. After topping treatment, the plants were kept for another 3 to 48 h in the growth chamber before sample collection.

Identification of miRNAs, Their Targets, and eTMs

The tobacco small-RNA data set and the approach reported in our previous study (Tang et al., 2012b) were used to identify miRNAs based on the newly available tobacco reference genome (Sierro et al., 2014). Targets of miRNAs were predicted using the Web-based tool psRNATarget with the default settings (Dai and Zhao, 2011), and the tobacco degradomic data set was further used to confirm the predictions using the method in our previous study (Tang et al., 2012b). Genes, i.e. QPT1 (AJ748262), *QPT2* (AJ748263), and *CYP82E4* (KC120817), involved in nicotine biosynthesis were based on previous studies (Dewey and Xie, 2013; Sierro et al., 2014). *NAC_148* (http://compsysbio.achs.virginia.edu/tobfac/; XM_009626731; Rushton et al., 2008), a NAC transcription factor that was responsive to topping in tobacco based on our unpublished results, was used as a positive control for the topping treatment in this study. Based on the publicly available EST and Plant Genome Database-assembled unique transcript databases and transcriptome (RNA sequencing) data of tobacco, we identified an eTM for nta-miRX27 in the intergenic region, which was named nta-eTMX27. The pipeline developed by our previous study (Ye et al., 2014) was used to predict eTMs for the miRNAs.

Phylogenetic Tree

Sequences of nta-miRX27 and its target *QPT2* and eTM (nta-eTMX27) were used as queries to search for their orthologs in the available genome sequences of two progenitors, *Nicotiana tomentosiformis* and *Nicotiana sylvestris*, as well as two other *Nicotiana* species, *Nicotiana benthamiana* and *Nicotiana otophora* (Bombarely et al., 2012; Sierro et al., 2013, 2014). Phylogenetic trees were

constructed using neighbor-joining method in MEGA6 with bootstrap 1,000 (Tamura et al., 2013).

Plasmid Constructs and Plant Transformation

The precursor sequence of nta-miRX27 was amplified from tobacco root DNA using a pair of primers containing *Bam*HI and *Sal*I site, respectively. To generate the nta-STTMX27-containing construct, a pair of back-to-back primers each containing a nta-miRX27 binding site with a central bulge, the 48-nucleotide oligonucleotide spacer sequence, and a *Bam*HI or *Sal*I restriction site (Supplemental Table S2) were used in PCR to generate a fragment containing two nta-miRX27 binding sites with the 48-nucleotide spacer in between. The fragment harboring nta-miRX27 or nta-STTMX27 was then subcloned into the binary vector pCHF3 between the *Bam*HI and *Sal*I sites and downstream of the *Cauliflower mosaic virus* 35S promoter to produce pCHF3-35S-nta-miRX27 and pCHF3-35S-nta-STTMX27, respectively.

The nta-eTMX27 sequence was amplified from tobacco root cDNA using a pair of primers, eTMX27-Full-F/eTMX27-Full-R, and the PCR products were subcloned into the binary vector pCHF3 to produce pCHF3-35S-nta-eTMX27. An RNAi construct containing an nta-eTMX27 inverted repeat sequence that was spaced by a soybean (*Glycine max*) intron was produced by overlapping PCR. The fragment of the nta-eTMX27 sense sequence was amplified with the eTMX27-A-F/eTMX27-intron-A-R primer pair and overlapped with the intron sequence amplified by eTMX27-intron-B-F/Intron-B-R primers. The overlapping product was cloned into pCHF3 between the *Sac*I and *Bam*HI sites to produce pCHF3-35S-nta-eTMX27-intron. The corresponding antisense nta-eTMX27 fragment was amplified with the primer pair eTMX27-C-F/eTMX27-C-R and subsequently cloned into pCHF3-35S-nta-eTMX27-intron between *Bam*HI and *Sal*I sites to produce the RNAi construct pCHF3-35S-dsNta-eTMX27. The *Agrobacterium tumefaciens*-mediated tobacco leaf disc transformation method was used to generate transgenic tobacco plants. Selection (on 200 μg mL^{-1} kanamycin media) of transformants and positive transgenic plants was performed as described previously (Li et al., 2014a). Primers used in PCR and RT-qPCR analyses are listed in Supplemental Table S2.

RT-qPCR Analysis

Total RNA was isolated from root samples of the control and topping-treated plants as well as various plant organ tissues using the Trizol reagent (Invitrogen). Three independent experiments, each consisting of at least three control and topping-treated plants, were used in quantification analyses. Expression levels of miRNA in root tissues were analyzed by RT-qPCR as described. Briefly, total RNA (1 μg) treated with RNase-free DNase I (Fermentas) was polyadenylated using *Escherichia coli* poly(A) polymerase (New England Biolabs). After phenol-chloroform extraction and ethanol precipitation, the RNAs were dissolved in RNase-free water. Reverse transcription was performed at 42°C for 30 min using a poly(T) adapter and Quantscript reverse transcriptase according to the manufacturer's instructions (Tiangen). RT-qPCR reactions were performed using a LightCycler 480 RT PCR instrument (Roche) and SYBR Green I Master Kit using a forward primer complementary to the miRNA and a universal reverse primer (miRNA-qPCR-R) complementary to the poly(T) adapter. Mitochondrial 5S RNA was used as an internal control for data normalization.

Quantification of the target genes and eTM was also carried out using RT-qPCR using a LightCycler 480 RT PCR instrument. One microgram of DNase I-treated total RNA was used in generating the first strand cDNA using an oligo(dT) primer and a reverse transcription kit with genome DNAse (Tiangen, KR106). The expression levels of nta-eTMX27 in different plant tissues were analyzed by semiquantitative PCR. *NtGAPDH* was used as a control in both qPCR and semiquantitative PCR.

RLM-5′ RACE Analysis

Total RNA was extracted from topping-treated plants at 48 h using a Trizol reagent (Invitrogen) as recommended by the manufacturer followed by further purification with an RNeasy Plant Mini Kit (QIAGEN). The purified RNA was treated by DNase I (Thermo Scientific) to eliminate possible DNA contamination and extracted using a standard phenol-chloroform method followed by ethanol precipitation. 5′-RACE was performed using the DNase-treated RNA and the SMARTer RACE cDNA Amplification Kit (Clontech). Reverse primers QPT2-1R-new or QPT2-2R-new (for the first nta-miRX27 target site) and QPT2-3R or QPT2-4R (for the second nta-miRX27 target site) were used in the respective reverse transcription reactions. Reverse-transcribed cDNAs were then used in the first round PCR reactions using the corresponding primer used in reverse transcription (i.e. QPT2-2R-new for the first nta-miRX27 target site and QPT2-4R for the second nta-miRX27 target site) in combination with the Universal Primer A Mix that anneals to the 5′ adaptor. The nested PCR was performed according to the manufacturer's instructions (Clontech) using a nested primer (i.e. QPT2-1R-new for the first nta-miRX27 target site and QPT2-3R for the second nta-miRX27 target site) in combination with the 5′-Nested Universal Primer. PCR products with expected size were gel purified and cloned to the pMD-18T vector (TakaRa). Clones with insert were sequenced using M13 primer. Sequencing results were analyzed using CLUSTALW (Thompson et al., 1994). Primers used in 5′ RACE are listed in Supplemental Table S2.

Nicotine Measurement

Fresh leaves were collected from the same positions of the topping-treated and control tobacco plants and dried at 105°C for 30 min and then 60°C for 3 d. Nicotine contents of the transgenic and control lines were measured in three biological samples, each with three technical replicates following the standard continuous flow protocol (YC/T160–2002) described by the State Tobacco Monopoly Administration of China.

Supplemental Data

The following supplemental materials are available.

Supplemental Figure S1. QPT2 gene annotation and validation of nta-miRX27-mediated cleavage of QPT2 by RLM-RACE.

Supplemental Figure S2. Validating nta-miRX27-mediated cleavage of the predicted target site using degradome data from roots of topping-treated tobacco plants.

Supplemental Table S1. Summary of novel miRNAs targeting the nicotine pathway genes.

Supplemental Table S2. Primers used in this study.

Received April 30, 2015; accepted August 3, 2015; published August 5, 2015.

LITERATURE CITED

Axtell MJ, Bowman JL (2008) Evolution of plant microRNAs and their targets. Trends Plant Sci **13:** 343–349

Baldwin IT (1999) Inducible nicotine production in native *Nicotiana* as an example of adaptive phenotypic plasticity. J Chem Ecol **25:** 3–30

Baldwin IT, Halitschke R, Kessler A, Schittko U (2001) Merging molecular and ecological approaches in plant-insect interactions. Curr Opin Plant Biol **4:** 351–358

Bartel DP (2004) MicroRNAs: genomics, biogenesis, mechanism, and function. Cell **116:** 281–297

Boke H, Ozhuner E, Turktas M, Parmaksiz I, Ozcan S, Unver T (2015) Regulation of the alkaloid biosynthesis by miRNA in opium poppy. Plant Biotechnol J **13:** 409–420

Bombarely A, Rosli HG, Vrebalov J, Moffett P, Mueller LA, Martin GB (2012) A draft genome sequence of *Nicotiana benthamiana* to enhance molecular plant-microbe biology research. Mol Plant Microbe Interact **25:** 1523–1530

Chen X, Xia J, Xia Z, Zhang H, Zeng C, Lu C, Zhang W, Wang W (2015) Potential functions of microRNAs in starch metabolism and development revealed by miRNA transcriptome profiling of cassava cultivars and their wild progenitor. BMC Plant Biol **15:** 33

Conkling MA, Cheng CL, Yamamoto YT, Goodman HM (1990) Isolation of transcriptionally regulated root-specific genes from tobacco. Plant Physiol **93:** 1203–1211

Dai X, Zhao PX (2011) psRNATarget: a plant small RNA target analysis server. Nucleic Acids Res **39:** W155–W159

Dewey RE, Xie J (2013) Molecular genetics of alkaloid biosynthesis in *Nicotiana tabacum*. Phytochemistry **94:** 10–27

Franco-Zorrilla JM, Valli A, Todesco M, Mateos I, Puga MI, Rubio-Somoza I, Leyva A, Weigel D, García JA, Paz-Ares J (2007) Target mimicry provides a new mechanism for regulation of microRNA activity. Nat Genet **39:** 1033–1037

Fu Y, Guo H, Cheng Z, Wang R, Li G, Huo G, Liu W (2013) NtNAC-R1, a novel NAC transcription factor gene in tobacco roots, responds to mechanical damage of shoot meristem. Plant Physiol Biochem **69:** 74–81

Gavilano LB, Coleman NP, Bowen SW, Siminszky B, Siminszky B (2007) Functional analysis of nicotine demethylase genes reveals insights into the evolution of modern tobacco. J Biol Chem **282:** 249–256

Heim WG, Sykes KA, Hildreth SB, Sun J, Lu RH, Jelesko JG (2007) Cloning and characterization of a *Nicotiana tabacum* methylputrescine oxidase transcript. Phytochemistry **68:** 454–463

Hibi N, Fujita T, Hatano M, Hashimoto T, Yamada Y (1992) Putrescine *N*-methyltransferase in cultured roots of *Hyoscyamus albus*: *n*-butylamine as a potent inhibitor of the transferase both in vitro and in vivo. Plant Physiol **100:** 826–835

Ivashuta S, Banks IR, Wiggins BE, Zhang Y, Ziegler TE, Roberts JK, Heck GR (2011) Regulation of gene expression in plants through miRNA inactivation. PLoS One **6:** e21330

Jones-Rhoades MW, Bartel DP, Bartel B (2006) MicroRNAS and their regulatory roles in plants. Annu Rev Plant Biol **57:** 19–53

Katoh A, Uenohara K, Akita M, Hashimoto T (2006) Early steps in the biosynthesis of NAD in Arabidopsis start with aspartate and occur in the plastid. Plant Physiol **141:** 851–857

Khraiwesh B, Zhu JK, Zhu J (2012) Role of miRNAs and siRNAs in biotic and abiotic stress responses of plants. Biochim Biophys Acta **1819:** 137–148

Li F, Huang C, Li Z, Zhou X (2014a) Suppression of RNA silencing by a plant DNA virus satellite requires a host calmodulin-like protein to repress RDR6 expression. PLoS Pathog **10:** e1003921

Li L, Eichten SR, Shimizu R, Petsch K, Yeh CT, Wu W, Chettoor AM, Givan SA, Cole RA, Fowler JE, et al (2014b) Genome-wide discovery and characterization of maize long non-coding RNAs. Genome Biol **15:** R40

Mallory AC, Bouché N (2008) MicroRNA-directed regulation: to cleave or not to cleave. Trends Plant Sci **13:** 359–367

Meng Y, Shao C, Wang H, Jin Y (2012) Target mimics: an embedded layer of microRNA-involved gene regulatory networks in plants. BMC Genomics **13:** 197

Naqvi AR, Sarwat M, Hasan S, Roychodhury N (2012) Biogenesis, functions and fate of plant microRNAs. J Cell Physiol **227:** 3163–3168

Ng DW, Zhang C, Miller M, Palmer G, Whiteley M, Tholl D, Chen ZJ (2011) *cis*- and *trans*-Regulation of miR163 and target genes confers natural variation of secondary metabolites in two *Arabidopsis* species and their allopolyploids. Plant Cell **23:** 1729–1740

Pasquinelli AE (2012) MicroRNAs and their targets: recognition, regulation and an emerging reciprocal relationship. Nat Rev Genet **13:** 271–282

Phillips JR, Dalmay T, Bartels D (2007) The role of small RNAs in abiotic stress. FEBS Lett **581:** 3592–3597

Rhoades MW, Reinhart BJ, Lim LP, Burge CB, Bartel B, Bartel DP (2002) Prediction of plant microRNA targets. Cell **110:** 513–520

Robert-Seilaniantz A, MacLean D, Jikumaru Y, Hill L, Yamaguchi S, Kamiya Y, Jones JD (2011) The microRNA miR393 re-directs secondary metabolite biosynthesis away from camalexin and towards glucosinolates. Plant J **67:** 218–231

Rushton PJ, Bokowiec MT, Han S, Zhang H, Brannock JF, Chen X, Laudeman TW, Timko MP (2008) Tobacco transcription factors: novel insights into transcriptional regulation in the Solanaceae. Plant Physiol **147:** 280–295

Saitoh F, Noma M, Kawashima N (1985) The alkaloid contents of sixty *Nicotiana* species. Phytochemistry **24:** 477–480

Shen D, Suhrkamp I, Wang Y, Liu S, Menkhaus J, Verreet JA, Fan L, Cai D (2014) Identification and characterization of microRNAs in oilseed rape (*Brassica napus*) responsive to infection with the pathogenic fungus *Verticillium longisporum* using *Brassica* AA (*Brassica rapa*) and CC (*Brassica oleracea*) as reference genomes. New Phytol **204:** 577–594

Sierro N, Battey JN, Ouadi S, Bakaher N, Bovet L, Willig A, Goepfert S, Peitsch MC, Ivanov NV (2014) The tobacco genome sequence and its comparison with those of tomato and potato. Nat Commun **5:** 3833

Sierro N, Battey JN, Ouadi S, Bovet L, Goepfert S, Bakaher N, Peitsch MC, Ivanov NV (2013) Reference genomes and transcriptomes of *Nicotiana sylvestris* and *Nicotiana tomentosiformis*. Genome Biol **14:** R60

Siminszky B, Gavilano L, Bowen SW, Dewey RE (2005) Conversion of nicotine to nornicotine in *Nicotiana tabacum* is mediated by CYP82E4, a cytochrome P450 monooxygenase. Proc Natl Acad Sci USA **102:** 14919–14924

Sinclair SJ, Murphy KJ, Birch CD, Hamill JD (2000) Molecular characterization of quinolinate phosphoribosyltransferase (QPRtase) in *Nicotiana*. Plant Mol Biol **44:** 603–617

Song W (1997) Molecular characterizations of two tobacco root-specific genes: TobRB7 and NtQPT1. PhD thesis. North Carolina State University, Raleigh, NC

Sunkar R, Zhu JK (2004) Novel and stress-regulated microRNAs and other small RNAs from *Arabidopsis*. Plant Cell **16:** 2001–2019

Tamura K, Stecher G, Peterson D, Filipski A, Kumar S (2013) MEGA6: molecular evolutionary genetics analysis version 6.0. Mol Biol Evol **30:** 2725–2729

Tang G, Yan J, Gu Y, Qiao M, Fan R, Mao Y, Tang X (2012a) Construction of short tandem target mimic (STTM) to block the functions of plant and animal microRNAs. Methods **58:** 118–125

Tang S, Wang Y, Li Z, Gui Y, Xiao B, Xie J, Zhu QH, Fan L (2012b) Identification of wounding and topping responsive small RNAs in tobacco (*Nicotiana tabacum*). BMC Plant Biol **12:** 28

Thompson JD, Higgins DG, Gibson TJ (1994) CLUSTAL W: improving the sensitivity of progressive multiple sequence alignment through sequence weighting, position-specific gap penalties and weight matrix choice. Nucleic Acids Res **22:** 4673–4680

Todesco M, Rubio-Somoza I, Paz-Ares J, Weigel D (2010) A collection of target mimics for comprehensive analysis of microRNA function in *Arabidopsis thaliana*. PLoS Genet **6:** e1001031

Wu HJ, Wang ZM, Wang M, Wang XJ (2013) Widespread long noncoding RNAs as endogenous target mimics for microRNAs in plants. Plant Physiol **161:** 1875–1884

Xie J, Song W, Maksymowicz W, Jin W, Cheah K, Chen W, Carnes C, Ke J, Conkling M (2004) Biotechnology: a tool for reduced risk tobacco products. The nicotine experience from test tube to cigarette pack. Rev. Adv. Tob. Sci. **30:** 17–37

Yan J, Gu Y, Jia X, Kang W, Pan S, Tang X, Chen X, Tang G (2012) Effective small RNA destruction by the expression of a short tandem target mimic in *Arabidopsis*. Plant Cell **24:** 415–427

Ye CY, Xu H, Shen E, Liu Y, Wang Y, Shen Y, Qiu J, Zhu QH, Fan L (2014) Genome-wide identification of non-coding RNAs interacted with microRNAs in soybean. Front Plant Sci **5:** 743

Zhang HB, Bokowiec MT, Rushton PJ, Han SC, Timko MP (2012) Tobacco transcription factors NtMYC2a and NtMYC2b form nuclear complexes with the NtJAZ1 repressor and regulate multiple jasmonate-inducible steps in nicotine biosynthesis. Mol Plant **5:** 73–84

Zhang YC, Liao JY, Li ZY, Yu Y, Zhang JP, Li QF, Qu LH, Shu WS, Chen YQ (2014) Genome-wide screening and functional analysis identify a large number of long noncoding RNAs involved in the sexual reproduction of rice. Genome Biol **15:** 512

Supplemental Figure S1

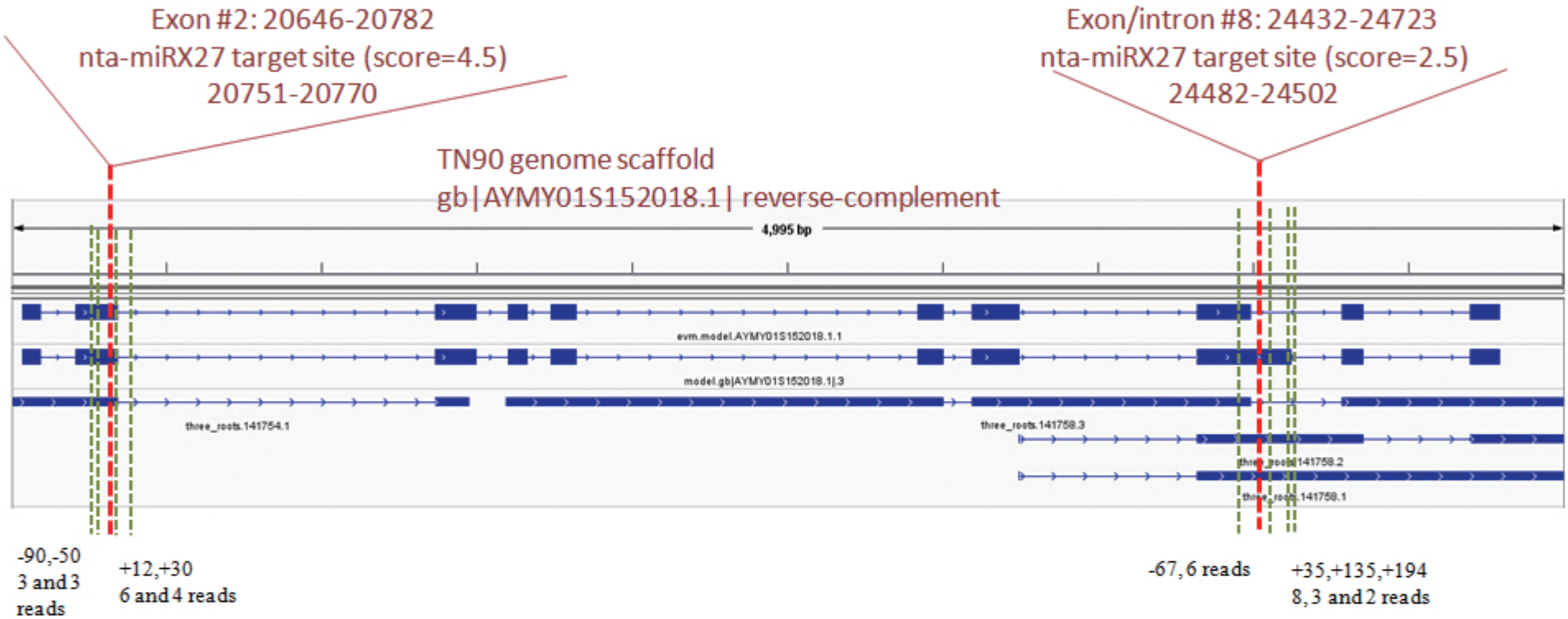

Figure S1. *QPT2* gene annotation and validation of nta-miRX27-mediated cleavage of *QPT2* by RLM-RACE. Gene annotation in NCBI (the first track) and the predicted gene structures of *QPT2* using Fgenesh (the second track), and assembled transcripts based on RNA-seq data from roots (SRX495526-7,9, Sierro et al., 2014) were shown. Two nta-miRX27 targeting sites were predicted (indicated by red lines) and the first targeting site located at exon #2 of *QPT2* was confirmed to be cleaved by nta-miRX27 based on our degradome data (Fig. S2) although none of the RLM-RACE products was mapped the expected cleavage position at both predicted targeting sites. The 5' end positions of the RLM-RACE products were indicated by dark yellow lines, their distances relative to the predicted cleavage sites and the corresponding number of clones at each position were shown at the bottom of the graph.

Supplemental Figure S2

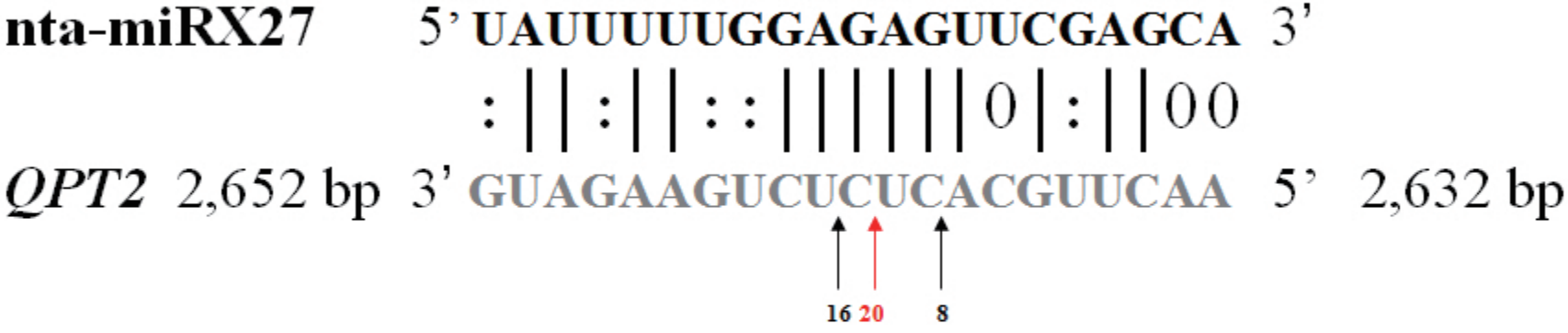

Figure S2. Validating nta-miRX27-mediated cleavage of the predicted target site (the first one at exon #2 in Fig. S1) using degradome data from roots of topping-treated tobacco plants. Base pairing between nta-miRX27 and its target *QPT2* is shown, in which a vertical line means a Watson-Crick pair, two dots represent a G-U pair and 0 represents mismatch. The numbers below the alignment indicate the numbers of degradomic reads at the positions indicated. The expected cleavage site is indicated by a red arrow.

Supplemental Table S1 :Summary of predicted and identified novel miRNAs targeting nicotine pathway genes

MiRNA accession	Mature sequences (5'-3')	Mature length	Precursor length	MFE/ kcal/ mol	Predicted target	Expression abundance (RPM*)		RT-qPCR analysis
						root	leaf	Root
nta-miRX13	AGTGTATAGCTATAAATAGGGACC	24	167	-90.8	PMT2	0.3	0.2	No
nta-miRX17	CCCCACTTGTGGGATTATACTGGG	24	153	-75.2	QPT1	0.5	2.5	Yes
nta-miRX19	CGGATCTCTTGGCGGAAAGAC	21	85	-40.6	NAC_148	4.5	5.6	Yes
nta-miRX20	CGTTGAAGTGGCAAGGATGAC	21	169	-76.4	CYP82E4	1.0	0.3	Yes
nta-miRX27	TATTTTTGGAGAGTTCGAGCA	21	131	-65.5	QPT2	0.5	22.0	Yes

Supplemental Table S1.Summary of predicted and identified novel miRNAs targeting nicotine pathway genes.*RPM: Repeat normalized reaSummary of predictSummary of predicted and identified novel miRNAs targeting nicotine pathway geneed and identified novel miRNAs

Supplemental Table S2 :Primers used in plasmid construction and other experiments in this study

Primer Name	Primer Sequence(5'—3')	Purpose
Poly(T) adapter	GCGAGCACAGAATTAATACGACTCACTATAGGTTTTTTTTTTTTVN	For miRNAs RT
RT-q-PCR-miR-R	GCGAGCACAGAATTAATACGAC	Universal Reverse primer for RT-qPCR analysis for nta-miRNAs
nta-miRX17-F [a]	CCCCACTTGTGGGATTATACTGGG	Relative RT-qPCR analysis ofnta-miRX17
nta-miRX27-F [a]	TATTTTTGGAGAGTTCGAGCA	Relative RT-qPCR analysis ofnta-miRX27
nta-miRX20-F [a]	CGTTGAAGTGGCAAGGATGAC	Relative RT-qPCR analysis ofnta-miRX20
nta-miRX19-F [a]	CGGATCTCTTGGCGGAAAGAC	Relative RT-qPCR analysis ofnta-miRX19
M-5S RNA-F	TAAGGTAGCGGCGAGACGAGC	Relative RT-qPCR analysis ofmitochondrial 5S RNA
NtGAPDH-q-F	GCAGTGAACGACCCATTTATCTC	Relative RT-qPCR analysis of NtGADPH
NtGAPDH-q-R	AACCTTCTTGGCACCACCCT	Relative RT-qPCR analysis of NtGADPH
QPT1-q-F	CTTAAGGGACTACTTTGAACTTATCC	Relative RT-qPCR analysis of QPT1
QPT1-q-R	CTAAAGAAACCTTGGTGCTGTAATTG	Relative RT-qPCR analysis of QPT1
QPT2-q-F	CCTTGAAGTTGGAAGGCGTAC	Relative RT-qPCR analysis of QPT2
QPT2-q-R	CATAAGGTTGGAAAGAGCCATCTG	Relative qRT-PCR analysis of QPT2
CYP82E4-q-F	CCACCGAAAATCCCCGGAGG	Relative RT-qPCR analysis of CYP82E4
CYP82E4-q-R	GGCGTCATTTGTAGAGAAACAGTC	Relative RT-qPCR analysis of CYP82E4
NAC_148-q-F	ACACGTTTATTCTAGAACCCGCC	Relative RT-qPCR analysis of NAC_148
NAC_148-q-R	GCAATTCCACCGCTGCCATTC	Relative RT-qPCR analysis of NAC_148
eTMX27-q-F	ATAGAAGCCGTTGGGGTAGTGAAC	Relative RT-qPCR analysis of eTMX27
eTMX27-q-R	ACTCATATCCTCGGGCGAACATC	Relative RT-qPCR analysis of eTMX27
eTMX27-Full-F [b]	CGGGATCCGTACGTGTTCTCGACTTTTC	pCHF3-35S-nta-eTMX27, for transgenic over-expression of nta-eTMX27
eTMX27-Full-R [b]	GCGTCGACCAATACACTCATAGACATTATAC	pCHF3-35S-nta-eTMX27, for transgenic over-expression of nta-eTMX27
eTMX27-A-F [b]	TCCGAGCTCGAAGCCGTTGGGGTAGTGAAC	pCHF3-35S-ds-nta-eTMX27, for transgenic down-regulation of nta-eTMX27
eTMX27-intron-A-R	ATCAGACTTACAACGTCGTGTGTGTCATTTTGACTG	pCHF3-35S-ds-nta-eTMX27, for transgenic down-regulation of nta-eTMX27
eTMX27-intron-B-F	CAGTCAAAATGACACACACGACGTTGTAAGTCTGAT	pCHF3-35S-ds-nta-eTMX27, for transgenic down-regulation of nta-eTMX27
Intron-B-R	GGATCCGCTCTATCTGCTGGGTCCAAATC	pCHF3-35S-ds-nta-eTMX27, for transgenic down-regulation of nta-eTMX27
eTMX27-C-F [b]	CGGGATCCCGTGTGTGTCATTTTGACTG	pCHF3-35S-ds-nta-eTMX27, for transgenic down-regulation of nta-eTMX27
eTMX27-C-R [b]	GCGTCGACGAAGCCGTTGGGGTAGTGAAC	pCHF3-35S-ds-nta-eTMX27, for transgenic down-regulation of nta-eTMX27
nta-miRX27-gene-F [b]	CGGGATCCCAAGCTATGTTGCTCGGAC	pCHF3-35S-nta-miRX27, for transgenic over-expression of nta-miRX27
nta-miRX27-gene-R [b]	GCGTCGACTGAGCTACGTTGCTCGAACTC	pCHF3-35S-nta-miRX27, for transgenic over-expression of nta-miRX27
STTMX27-F[a,c]	CGGGATCC,TGCTCGAACTCCTATCCAAAAATAGTTGTTGTTGTTATGG	pCHF3-35S-STTMX27, for transgenic destruction of nta-miRX27
STTMX27-R[a,c]	GCGTCGAC,TATTTTTGGATAGGAGTTCGAGCAATTCTTCTTCTTTAGACCA	pCHF3-35S-STTMX27, for transgenic destruction of nta-miRX27
STTM-48 nt	GTTGTTGTTGTTATGGTCTAATTTAAATATGGTCTAAAGAAGAAGAAT	As STTMX27 template
QPT2-1R-New	CGCCATCATTTACATACCACTCCAC	5'RACE analysis for the first cleavage site of QPT2
QPT2-2R-New	CCAAGATGTAAGCAGGGTGTG	5'RACE analysis for the first cleavage site of QPT2
QPT-3R	CTTCCAACTTCAAGGGCGAGC	5'RACE analysis for the second cleavage site of QPT2
QPT-4R	GCTCATGCTCGTTTTGTACGCC	5'RACE analysis for the second cleavage site of QPT2

Supplemental Table S2.Primers used in plasmid construction and other experiments in this study.[a], MiRNAequence is underlined; [b], Restriction site used for cloning is underlined; [c], STTM mimic sequence is underlined.

4